

## *Original*

Dangendorf, S.; Rybski, D.; Mudersbach, C.; Mueller, A.; Kaufmann, E.;  
Zorita, E.; Jensen, J.:

### **Evidence for long-term memory in sea level**

In: Geophysical Research Letters (2014) AGU

DOI: 10.1002/2014GL060538



## RESEARCH LETTER

10.1002/2014GL060538

## Key Points:

- We find evidence for long-term memory in MSL records
- Long-term memory is found in the steric and mass components
- This natural variability produces climate internal multidecadal trends

## Supporting Information:

- Readme
- Text S1
- Figure S1
- Figure S2
- Figure S3
- Figure S4
- Figure S5
- Figure S6

## Correspondence to:

S. Dangendorf,  
soenke.dangendorf@uni-siegen.de

## Citation:

Dangendorf, S., D. Rybski, C. Mudersbach, A. Müller, E. Kaufmann, E. Zorita, and J. Jensen (2014), Evidence for long-term memory in sea level, *Geophys. Res. Lett.*, *41*, 5530–5537, doi:10.1002/2014GL060538.

Received 14 MAY 2014

Accepted 7 JUL 2014

Accepted article online 12 JUL 2014

Published online 5 AUG 2014

## Evidence for long-term memory in sea level

Sönke Dangendorf<sup>1</sup>, Diego Rybski<sup>2</sup>, Christoph Mudersbach<sup>3</sup>, Alfred Müller<sup>4</sup>, Edgar Kaufmann<sup>4</sup>, Eduardo Zorita<sup>5</sup>, and Jürgen Jensen<sup>1</sup>

<sup>1</sup>Research Institute for Water and Environment, University of Siegen, Siegen, Germany, <sup>2</sup>Group of Climate Change and Development, Potsdam Institute for Climate Impact Research, Potsdam, Germany, <sup>3</sup>Institute for Hydrology and Environment, Bochum University of Applied Sciences, Bochum, Germany, <sup>4</sup>Department of Mathematics, University of Siegen, Siegen, Germany, <sup>5</sup>Institute for Coastal Research, Helmholtz-Centre Geesthacht, Geesthacht, Germany

**Abstract** Detection and attribution of anthropogenic climate change signals in sea level rise (SLR) has experienced considerable attention during the last decades. Here we provide evidence that superimposed on any possible anthropogenic trend there is a significant amount of natural decadal and multidecadal variability. Using a set of 60 centennial tide gauge records and an ocean reanalysis, we find that sea levels exhibit long-term correlations on time scales up to several decades that are independent of any systematic rise. A large fraction of this long-term variability is related to the steric component of sea level, but we also find long-term correlations in current estimates of mass loss from glaciers and ice caps. These findings suggest that (i) recent attempts to detect a significant acceleration in regional SLR might underestimate the impact of natural variability and (ii) any future regional SLR threshold might be exceeded earlier/later than from anthropogenic change alone.

## 1. Introduction

The state of the global mean sea surface height is mainly determined by volumetric expansion and contraction driven by density variations and mass exchange with terrestrial freshwater storages. The recent state of scientific knowledge suggests that sea levels have changed in response to global mean temperature for millions of years, with epochs exceeding the present-day mean sea level (MSL) by 5 to 10 m [Church *et al.*, 2013]. There is also high confidence from proxy and instrumental sea level records that the current global MSL rise has started to accelerate at the end of the nineteenth century relative to the low rates of rise during the last two millennia with likely highest rates during the past two decades [Church *et al.*, 2013]. Due to the delayed response to the past [Levermann *et al.*, 2013] and future [Slangen *et al.*, 2014] temperature changes, it is expected that these high rates will at least continue or even increase. Any further rise in global or regional MSL exacerbates the risk of flooding for highly populated coastal areas and requires profound adaption strategies [Hallegatte *et al.*, 2013; Boettle *et al.*, 2013]. This has motivated a number of scientists to search for already present significant accelerations which could be attributed to anthropogenic climate change [e.g., Jevrejeva *et al.*, 2006; Woodworth *et al.*, 2009; Houston and Dean, 2011; Sallenger *et al.*, 2012; Calafat and Chambers, 2013]. A major challenge consists in distinguishing between natural variations and a comparably small externally forced anthropogenic signal [Haigh *et al.*, 2014], especially when analyzing historical records from geological surveys [Rohling *et al.*, 2013].

A key question when searching for accelerations is whether the detected signal is statistically significantly different to what has been observed before the Anthropocene when the man-made contribution to climate change was absent [e.g., Gehrels and Woodworth, 2013]. This has been mostly tackled under the assumption that the residuals (the noise) around the signal (the trend or acceleration) are identically distributed and are either independent or exhibit short-term correlations which can be approximated by a first-order autoregressive (AR1) process. However, from other climatic observations, such as temperature [Koscielny-Bunde *et al.*, 1998] or run-off records [Kantelhardt *et al.*, 2006], it is known that although noise may be normally distributed, there is also evidence for persistence on longer time scales up to at least 200 years (this has been demonstrated in observations, millennial proxies, and simulations [Rybski *et al.*, 2008; Franzke, 2012a]). Although the mechanisms behind the phenomenon remain unclear (some authors attribute the memory to the heat storage capacity of the ocean [e.g., Monetti *et al.*, 2003]), its presence highlights that testing for significance in such long-term-correlated records requires a more sophisticated statistical handling [Franzke, 2012b]. Since persistence naturally leads to longer periods of high or low stands [Lennartz and Bunde, 2009], an increasing

tendency might—under the assumption of white or AR1 noise—be erroneously attributed to anthropogenic forcing. Additionally, such persistence can reinforce the deterministic sea level rise over extended periods with severe impacts for coastal regions. Hence, an improved understanding of such time series structures and their underlying physics is indispensable for both: detection and attribution of anthropogenic signals [e.g., *Calafat and Chambers*, 2013] as well as estimating uncertainties of future sea level projections.

Here we apply the well-established Detrended Fluctuation Analysis (DFA) [Peng *et al.*, 1994; Bunde *et al.*, 2000] to investigate the correlation structure of sea level records. We consider three different sources of information: long and homogeneous tide gauge (TG) records [Holgate *et al.*, 2013], monthly fields of an ocean reanalysis covering the period from 1871 to 2008 [Carton and Giese, 2008], and recent estimates for mass loss from glaciers and ice sheets [Box, 2013; Marzeion *et al.*, 2012]. We search in each time series for the existence of long-term persistence (LTP). Since sea levels are an integrative measure driven by various physical processes, we will also examine whether the steric component (i.e., density (temperature and salinity)-driven variations), which is known to be closely linked to decadal fluctuations of sea level rise (SLR) [Stammer *et al.*, 2013], drives the temporal and spatial correlation structure of regional sea levels. Finally, we will explore the differences between MSL and the steric component and compare them with mass contributions from glaciers and the Greenland ice sheets.

## 2. Data and Methods

We analyze monthly averaged TG data from the archive of the Permanent Service of Mean Sea Level (PSMSL) [Holgate *et al.*, 2013]. Since we are interested in identifying LTP, we use only long (>90 years over the period from 1871 to 2008) and continuous (less than 25% missing values) records from the revised local reference subset. To avoid considerable spatial heterogeneity, some records from more densely sampled regions such as the North and Baltic Sea were excluded. Data gaps smaller than 3 months were filled by applying cubic spline interpolation. All records were corrected for the inverted barometer effect, i.e., the hydrostatic response of the ocean to pressure fluctuations was accounted for (note that the impact of this correction on the scaling behavior is negligible as demonstrated in Figure S2 and Text S1 in the supporting information). To consider vertical land motion, each record was also corrected for the effect of glacial isostatic adjustment by using the numbers provided by Peltier [2004] (note that the correction does not affect the results of the DFA2, since DFA2 removes linear trends from the data). Our final TG data set consists of 60 records, which are shown and listed in the supporting information (Figure S1 and Table S1).

The steric component was obtained from the last version (2.2.4) of the Simple Ocean Data Assimilation (SODA) [Carton and Giese, 2008]. SODA is an ocean model with a horizontal resolution of  $0.25^\circ \times 0.4^\circ$  and 40 vertical levels covering the entire global ocean. It is forced with ensemble mean atmospheric fields from the Twentieth Century Reanalysis Project [Compo *et al.*, 2011] and assimilates water temperature and salinity observations. Since the model is based on the Boussinesq approximation, it conserves volume but not mass. To account for missing steric effects, a spatially uniform global mean of the steric height calculated from density fields referenced down to the ocean bottom (in the model) was added at each time step [Greatbach, 1994]. Nevertheless, mass changes resulting from freshwater exchange between the land and the ocean are still missing. To account for different components of steric sea level, we divide the SODA sea level into five different measures: dynamic height (sea surface height), steric height (locally vertically integrated), thermosteric height (locally vertically integrated), halosteric height (locally vertically integrated), and ocean bottom pressure (dynamic height minus steric, hereafter OBP).

Comprehensive records of mass loss from glaciers and ice sheets covering the period of interest for the present study are not available. Therefore, we analyze centennial reconstructions established via the correlations between ice melting and climatic measurements. For instance, for the Greenland ice sheet, Box [2013] reconstructed the surface mass balance (SMB) from surface air temperature and precipitation observations over the period from 1840 to 2012. Marzeion *et al.* [2012] provided an annual record of the global sea level contribution from glaciers over the twentieth century. The glacier contribution was also calculated from temperature and precipitation observations and covers a period from 1902 to 2009. Both records are integrated into the analysis as independent measures of LTP in the mass component of sea level.

As motivated in section 1, we are interested in the temporal correlation characteristics of sea level on time scales up to several decades. In contrast to the exponential decay of a classical AR1 process, LTP causes a

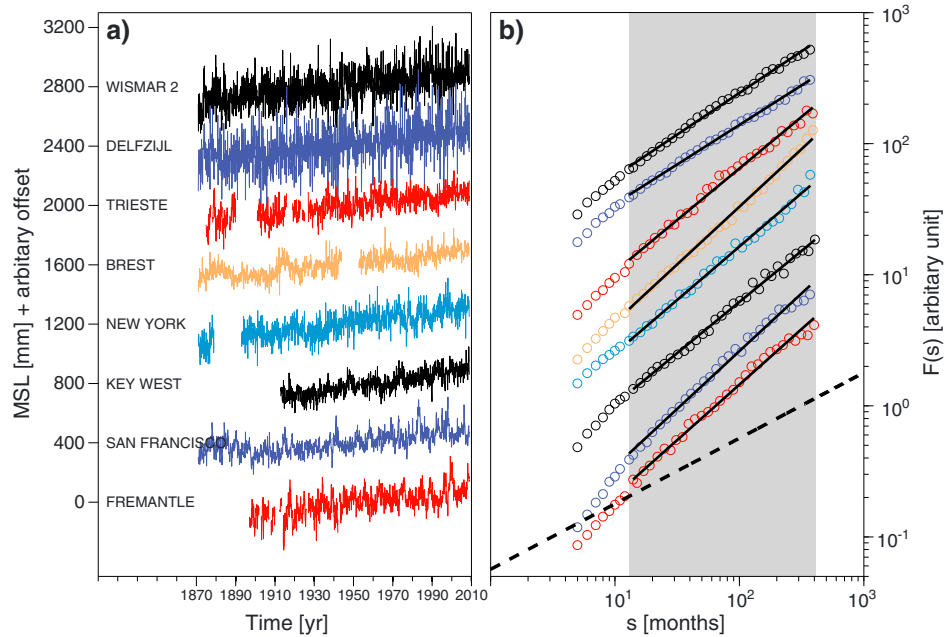


**Figure 1.** (a) Time series of eight selected TGs from around the world. All time series have been corrected for the mean seasonal cycle and, if significant (here Fremantle and San Francisco), also for the quasi-oscillatory El Niño–Southern Oscillation (ENSO) influence (see supporting information). (b) Fluctuation functions of the eight records calculated with DFA2. The black dashed line marks the exponent  $\alpha = 0.5$ , i.e., uncorrelated noise. The grey-shaded area displays the window for which the  $\alpha$  value has been estimated ( $13 \leq s \leq 414$  months).

power law decay of the autocorrelation function  $C(s)$ . The evaluation of  $C(s)$  itself is difficult, as it is very noisy for large time lags  $s$ . Moreover, trends in the analyzed records hinder a reliable characterization. A more sophisticated way for analyzing LTP of geophysical time series is DFA [e.g., *Kantelhardt et al., 2001*]. First, a random walk time series  $Y(i)$  (i.e., the cumulative sum of the original record) is calculated. Second, the time series is divided into  $N_s = N/s$  nonoverlapping segments, each containing  $s$  points. For each segment a polynomial trend of the order  $n$  (here 2, therefore DFA2) is estimated and removed. Third, the variance  $Y_s$  is calculated for each segment, the average is taken over all segments, and the root-mean-square is computed to obtain the fluctuation function  $F(s)$ : (Here we use segments defined starting from the beginning and the end of the time series. Thus, we get  $2N_s$  segments for each  $s$  [see also *Kantelhardt et al., 2001*].)

$$F(s) = \left[ \frac{1}{2N_s} \sum_{v=1}^{2N_s} \left( \frac{1}{s} \sum_{i=1}^s Y_s^2[(v-1)s+i] \right) \right]^{\frac{1}{2}} \tag{1}$$

The LTP can then be estimated as the asymptotic slope  $\alpha$  of  $F(s)$  in the double logarithmic representation. A time series is uncorrelated or has only short-term memory when  $\alpha = 0.5$ , long-term correlated when  $\alpha > 0.5$ , and long-term correlated and nonstationary (fractional Brownian motion) when  $\alpha > 1.0$  [*Peng et al., 1994*]. DFA is similar to Hurst R/S Analysis [*Hurst, 1951*], but DFA2 removes linear trends in the original records (quadratic trends need to be very strong to affect the fluctuation function [*Kantelhardt et al., 2001*]).

The accuracy of  $F(s)$  decreases with the ratio  $N/s$ , and therefore,  $s$  should generally be smaller than  $N/4$  [*Rybski et al., 2008*]. Here we focus on the period from 1871 to 2008. Data gaps are handled by merging the fragments, which turns out to have negligible effects on the estimation of  $\alpha$  [*Chen et al., 2002*]. We are therefore able to estimate LTP on time scales up to  $\sim 35$  years ( $13 \leq s \leq 414$  months). To avoid biases resulting from oscillatory behavior [*Kantelhardt et al., 2001*] in the time series, the mean seasonal cycle is removed prior to any further analyses (see also supporting information section S1). In some records from the Pacific quasi-oscillatory signals in frequency bands between 3 and 7 years are evident; these are also removed (see Text S1, Figures S3 and S4, and section S2 of the supporting information). Uncertainties (95% confidence) of  $\alpha$  are estimated in a nonparametric frame of computing 1000 surrogate time series using the standard Fourier-Filter method [e.g., *Kantelhardt et al., 2001*] for each specific  $\alpha$  and  $13 \leq s \leq 414$  months. A plot summarizing the simulation

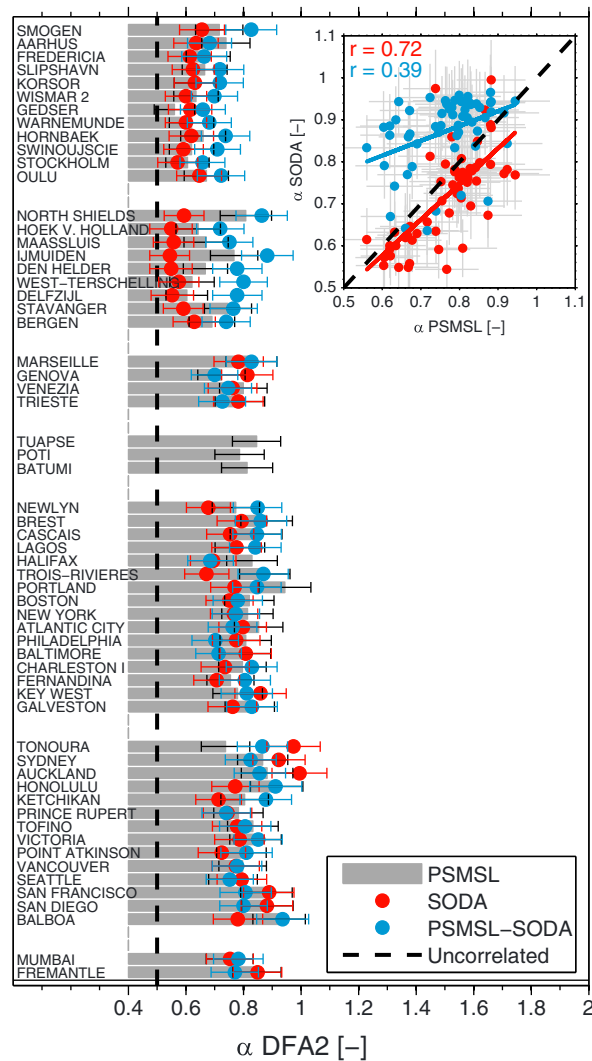


**Figure 2.** The  $\alpha$  exponents estimated with DFA2 for 60 tide gauge records (grey), their related SODA counterparts (red, steric sea level), and difference between tide gauge and SODA output (blue). Uncertainties are given by error bars. The black dashed line shows the exponent  $\alpha=0.5$ , indicating uncorrelated noise. The inset shows the correlation between  $\alpha$  values estimated with DFA2 from TG records, their corresponding SODA counterparts, and the residuals. The tide gauges are grouped (from top to bottom): Baltic Sea, North Sea, Mediterranean, Black Sea, Atlantic Ocean, Pacific Ocean, and Indian Ocean. Note that the Black Sea is not resolved by the SODA model.

in shelf regions, water levels are highly affected by local disturbances in the atmosphere. This forcing is mostly barotropic in nature and results in up to 3 times larger variability than elsewhere in the ocean. It explains up to 90% of the intraannual variability [e.g., Dangendorf et al., 2014] and can therefore be understood as a white noise process superimposed onto the slow processes acting in the deeper ocean. As recently analytically explored by Ludescher et al. [2011], adding white noise to a long-term-correlated time series might result in a reduction of  $\alpha$ .

The results from the 60 TG records are compared to the dynamic height derived from the SODA reanalysis for the grid point with the highest correlation within  $2^\circ \times 2^\circ$  around the TG site (seasonal cycle removed analogously). The skill of the SODA reanalysis for investigating long-term variations in sea level has previously

results for the methodological fitting uncertainties of  $\alpha$  values between 0.5 and 1 can be found in the supporting information (Figure S5).

### 3. Results

To test whether sea level exhibits LTP, we first apply DFA2 to the monthly TG records. Figure 1a shows, as an example, eight arbitrarily selected time series from TGs distributed around the globe. Despite some differences in subseasonal noise characteristics (e.g., large variability in North and Baltic Sea records due to the influence of strong winds over the continental shelf [Dangendorf et al., 2013]), all records exhibit pronounced irregular fluctuations on all scales with persistent multidecadal excursions from the mean state. This visual indication of LTP is confirmed by the fluctuation function of each of the eight records (Figure 1b). In the double logarithmic representation, all fluctuation functions are approximately straight lines for  $s > 12$  month, with slopes far beyond  $\alpha = 0.5$  of uncorrelated noise. This indicates that in addition to the persistence present on short time scales [Church and White, 2011], there is also significant LTP on time scales at least up to  $\sim 35$  years. Figure 1 further suggests that records from semienclosed basins or the continental shelf (Wismar, Delfzijl, and Trieste) are characterized by smaller slopes ( $\alpha = 0.6-0.8$ ) compared to records from coastlines of the large ocean basins (e.g., Brest, San Francisco, and Fremantle;  $\alpha = 0.8-0.95$ ).

This is confirmed by the results from all 60 records (Figure 2). The differences between semienclosed basins and the open ocean are particularly striking for the North and Baltic Sea areas. Due to the shallow water depths and the huge atmospheric variability

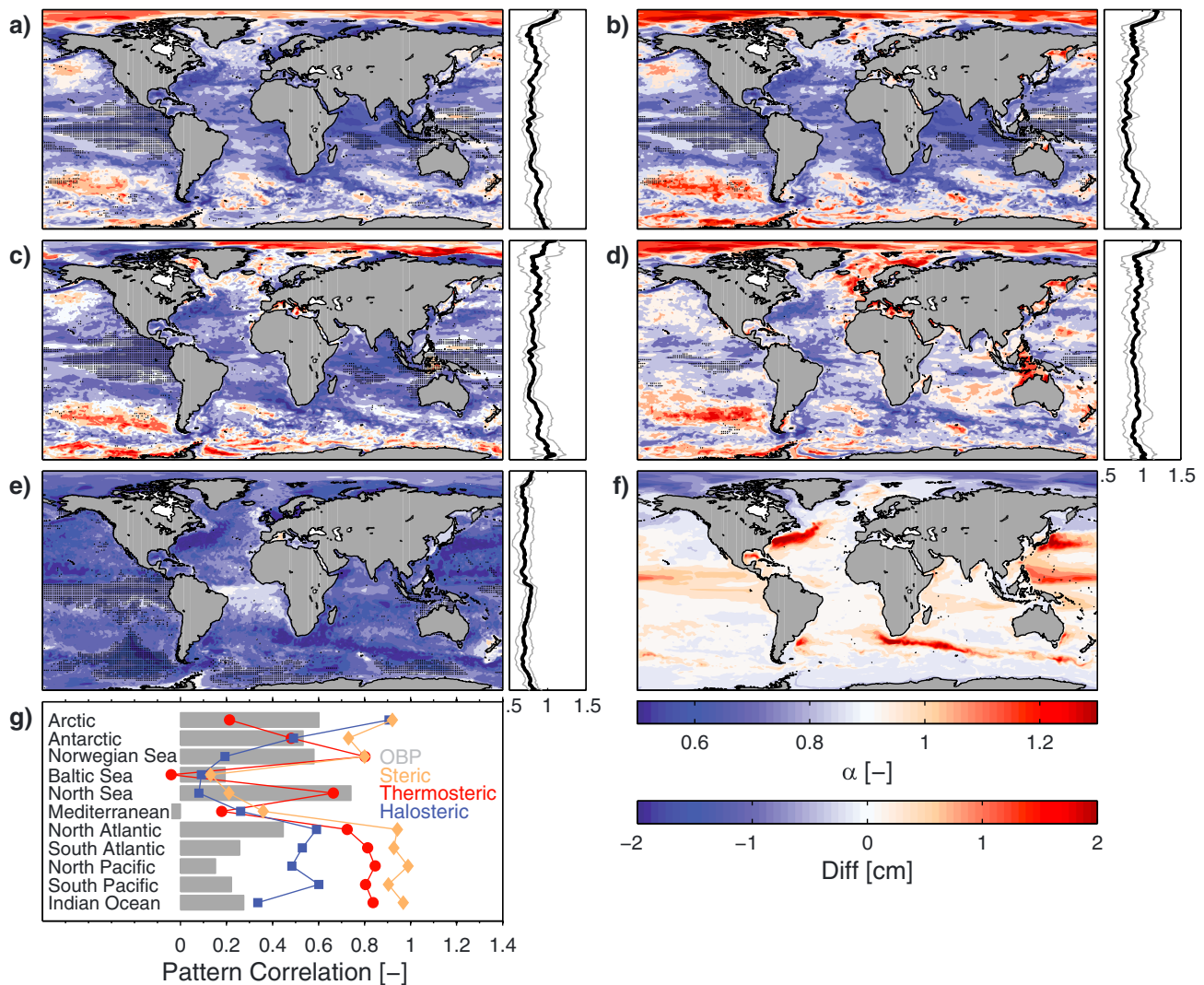


**Figure 3.** The  $\alpha$  values estimated with DFA2 for the SODA reanalysis grid points and the period 1871 to 2008: (a) dynamic height, (b) steric height, (c) thermosteric height, (d) halosteric height, and (e) ocean bottom pressure. The  $\alpha$  values were estimated for windows from 13 to 414 months. Locations for which the ENSO influence was removed are marked by a black dot. The subplots on the right represent the latitudinal average (black) and the respective standard deviation (grey). (f) Differences between the standard deviations of the thermosteric and halosteric height. Figure 3e shows the pattern correlation for different ocean basins calculated between the dynamic height and the contributions coming from the steric height (yellow), the thermosteric height (red), the halosteric height (blue), and ocean bottom pressure (grey).

been demonstrated by *Chepurin et al.* [2014] and *Calafat et al.* [2014] and was independently validated for the present study for frequency bands from 13 to 414 months (Figure S5 in the supporting information). The  $\alpha$  values for the dynamic height from SODA grid points representative of the TG sites are also shown in Figure 2 and agree reasonably well with those derived from the TG records ( $r=0.72$ ; inset of Figure 2). The main features, such as the differences between different basins, are mostly captured by the model. This indicates that a considerable part of the LTP found in the TG records is likely related to density-driven variations. Especially on regional scales, this could be expected, since much of the temporal variability is driven by thermal adjustment processes in response to changing winds [*Calafat and Chambers, 2013*] or buoyancy forcing [*Piecuch and Ponte, 2012*]. At some stations, however, large differences between the exponents exist and will be explored below.

The spatial distribution of LTP in the dynamic height as derived from all SODA model grid points is depicted in Figure 3. LTP is significant in the majority of the global ocean with  $\alpha$  values mostly between 0.6 and 0.95. There is also a weak latitudinal dependence with slightly larger  $\alpha$  values in high latitudes. For instance, values

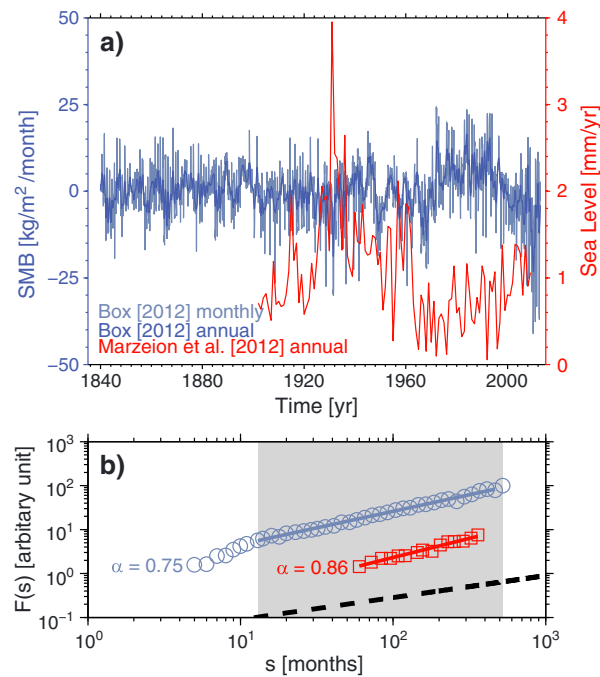


**Figure 4.** (a) Time series of Greenland's monthly surface mass balance (SMB, blue) [Box, 2012] and the annual sea level contribution estimated for the world's glaciers (red) [Marzeion et al., 2012]. (b) The corresponding fluctuation functions. The grey-shaded area shows the frequency bands for which the  $\alpha$  value has been estimated ( $13 \leq s \leq 414$  months). The black dashed line in Figure 4b marks the exponent  $\alpha = 0.5$ , i.e., uncorrelated noise.

shelf regions (North Sea and Baltic Sea). The latter suggests that the LTP characteristics over the continental shelves are mainly a footprint of wind-driven redistribution. Focusing on the steric component, it is obvious that thermosteric sea level dominates the picture over large parts of the open ocean (e.g., Atlantic, Pacific, and Indian Ocean), while the halosteric component determines the LTP structure in the Arctic Ocean. A balanced relationship is found in the Antarctic region. These basin-internal features are closely linked to the ratio between thermosteric and halosteric sea level variability (Figure 3f). In regions, where the variability of the thermosteric contribution is larger, it also dominates the spatial patterns of  $\alpha$ ; the same is true for the halosteric component.

Although the steric component accounts for a major fraction of the LTP in regional sea level, some differences remain unexplained. This poses the question where the missing part is coming from. To explore this in more detail, we subtract the steric signals from all TG records and search for LTP in the residuals (Figure 2). The latter contain contributions such as the mass contribution from glaciers and ice caps as well as model or measurement errors. At all sites the residuals still exhibit a clear scaling behavior, suggesting that the LTP in sea level is also driven by mass changes coming from the cryosphere (although the spatial dependence is more related to the steric component, see inset of Figure 2). To underpin this hypothesis, we additionally analyze two century-scale reconstructions of SMB of the Greenland ice sheet [Box, 2013] and the world's glacier contribution to sea level rise [Marzeion et al., 2012] in a similar way as it was done for TG records and steric sea level (Figure 4). For both records we find persistence, with  $\alpha$  values of 0.75 and 0.86 for Greenland's SMB and the glacier contribution, respectively. Since melting rates of the large ice sheets and glaciers are strongly governed by the regional climate (e.g., surface melting in response to temperature fluctuations, precipitation, or atmospheric circulation) and the ocean (ice calving), which are in turn both characterized by a clear scaling behavior [e.g., Bunde et al., 2014; Franzke, 2012a], a LTP fingerprint in the mass component of sea level is likely. This confirms that LTP (on various time scales) in sea level is driven by different factors.

exceeding  $\alpha = 1$  are found over large parts of the Arctic Ocean, pointing to the existence of a nonstationary behavior in these regions. Fluctuation exponents larger than 1 are also identified in parts of the North and South Pacific. In regions of strong currents (e.g., Gulf Stream and Kurisho Current),  $\alpha$  values are smaller, which is opposite to the finding for surface temperature from a global climate model in Rybski et al. [2008]. This may be explained by the larger uncertainties in the SODA model in these regions [Calafat et al., 2014].

To explore which mechanisms control the regional LTP imprints of the dynamic height, we also calculated  $\alpha$  values for each contributing factor (Figures 3b–3e) and compared the maps derived for different ocean basins via centered pattern correlation (Figure 3g), which refers to the correlation of deviation patterns, where the spatial mean has been subtracted [Barkhordarian et al., 2012]. The results point to a dominant influence of density (thermosteric and halosteric)-driven sea level changes in the deep ocean, while OBP variations are the main driver of the spatial LTP characteristic in shallow continental

#### 4. Discussion

In the present study we have reassessed the role of internal climate variability on regional sea level rise. By applying DFA2 we have demonstrated that contrary to the widespread assumption that sea levels are governed by short-term correlations [e.g., Church and White, 2011], they also exhibit a nonnegligible fraction of long-term internal climate variability, which is partly related to the inertia of the global ocean. While this perspective has got less attention in the sea level community so far, it is well established in other fields of climate science. For instance, it is well known that global and regional temperature time series show LTP on time scales up to 200 years [Rybski et al., 2008] (this is true for proxies as well as millennial forced and control simulations of climate models). It has also been demonstrated that temperature records over the ocean exhibit stronger LTP than continental stations [Eichner et al., 2003], a feature that has been linked with the large heat storage capacity of the ocean. As our results point to larger LTP in sea level than found in continental temperature records, the presented findings confirm the common assumption that much of the multidecadal Earth's climate and variability is shaped by the ocean [Trenberth, 2010].

The finding that sea levels exhibit scaling behavior induced by various forcing factors shows that estimating linear or nonlinear trends requires more complex null models [e.g., Franzke, 2012b] than previously suggested. Obviously, the persistence of sea level on long time scales will increase the standard error calculated as a measure of significance from residuals around an estimated signal [Rybski and Bunde, 2009; Lennartz and Bunde, 2009; Bos et al., 2014]. Although it is unlikely that the use of more sophisticated null models will affect the conclusion that sea levels are rising significantly since the late nineteenth century [Gehrels and Woodworth, 2013], it will affect the conclusions regionally drawn from shorter records spanning only over a few decades.

The presence of LTP in sea level records also has far reaching consequences for the crucial question of whether the rate of SLR is currently significantly accelerating or not. The detection of suchlike behavior [Haigh et al., 2014] and its attribution to external forcing is vital due to the potentially large impacts on coastal zones. To this end it is important to notice that the steric component of SLR in climate simulations up to 2100 only shows a clear acceleration for the high-emission scenarios, whereas the rate remains close to linear for moderate- and low-emission scenarios [Church et al., 2013]. An acceleration is expected for the contribution coming from ice melting of land-locked ice. This, however, is not incorporated into the latest generation of models and calculated "offline." Even combining both contributions does only suggest a significant acceleration after the 2020s [Haigh et al., 2014]. The detection of acceleration during the twentieth or the early 21st century would therefore indicate that future SLR may attain much higher values than those simulated by climate models (at least globally). So far, the presence of acceleration has been attributed to the external anthropogenic forcing. Our results suggest that due to the naturally pronounced mountain valley structure on all scales, a stochastic acceleration in sea level could be wrongly interpreted as deterministic, leading to biased extrapolation of the present SLR into the future.

#### Acknowledgments

All data sets used in the present study are online accessible from PSMSL (<http://www.psmsl.org/>), 20CR ([http://www.esrl.noaa.gov/psd/data/gridded/data.20thC\\_ReanV2.html](http://www.esrl.noaa.gov/psd/data/gridded/data.20thC_ReanV2.html)), SODA (<http://iridl.ldeo.columbia.edu/SOURCES/CARTON-GIESE/SODA/>), glacier SLR contribution ([www.the-cryosphere.net/6/1295/2012/tc-6-1295-2012-supplement.zip](http://www.the-cryosphere.net/6/1295/2012/tc-6-1295-2012-supplement.zip)), and SMB (<http://polarmet.osu.edu/jbox/data/smb/>). We thank Ben Marzeion, Jason Box, the 20CR team, the PSMSL team, and the SODA team for sharing their data without any charge. We are grateful to Thomas Wahl and Francisco Calafat, who provided useful comments on an earlier version of the manuscript. We further acknowledge Victor Ocana for sharing his manuscript "Stochastic trends in sea level rise," which has been submitted recently for peer review. This work was funded by an internal funding for multidisciplinary science at the University of Siegen.

The Editor thanks two anonymous reviewers for their assistance in evaluating this paper.

#### References

- Barkhordarian, A., J. Bhend, and H. von Storch (2012), Consistency of observed near surface temperature trends with climate change projections over the Mediterranean region, *Clim. Dyn.*, *38*, 1695–1702.
- Boettle, M., D. Rybski, and J. P. Kropp (2013), How changing sea level extremes and protection alter coastal flood damages, *Water Resour. Res.*, *49*, 1199–1210, doi:10.1002/wrcr.20108.
- Bos, M. S., S. D. P. Williams, I. B. Araujo, and L. Bastos (2014), The effect of temporal correlated noise on the sea level rate and acceleration uncertainty, *Geophys. J. Int.*, *196*, 1423–1430.
- Box, J. E. (2013), Greenland ice sheet mass balance reconstruction. Part II: Surface mass balance (1840–2010), *J. Clim.*, *26*, 6974–6989.
- Bunde, A., S. Havlin, J. W. Kantelhardt, T. Penzel, J. H. Peter, and K. Voigt (2000), Correlated and uncorrelated regions in heart-rate fluctuations during sleep, *Phys. Rev. Lett.*, *85*, 3736–3736.
- Bunde, A., J. Ludescher, C. L. E. Franzke, and U. Büntgen (2014), How significant is West Antarctic warming?, *Nat. Geosci.*, *7*, 246–247.
- Calafat, F. M., and D. P. Chambers (2013), Quantifying recent acceleration in sea level unrelated to internal climate variability, *Geophys. Res. Lett.*, *40*, 3661–3666, doi:10.1002/grl.50731.
- Calafat, F. M., D. P. Chambers, and M. N. Tsimplis (2014), On the ability of global sea level reconstructions to determine trends and variability, *J. Geophys. Res. Oceans*, *119*, 1572–1592, doi:10.1002/2013JC009298.
- Carton, J. A., and B. S. Giese (2008), A reanalysis of ocean climate using Simple Ocean Data Assimilation (SODA), *Mon. Weather Rev.*, *136*, 2999–3017.
- Chen, Z., P. C. Ivanov, K. Hu, and H. E. Stanley (2002), Effect of nonstationarities on detrended fluctuation analysis, *Phys. Rev. E*, *65*, 041107.
- Chepurin, G. A., J. A. Carton, and E. Leuliette (2014), Sea level in ocean reanalyses and tide gauges, *J. Geophys. Res. Oceans*, *119*, 147–155, doi:10.1002/2013JC009365.

- Church, J. A., and N. J. White (2011), Sea-level rise from the late 19th to the early 21st century, *Surv. Geophys.*, 32(4–5), 585–602, doi:10.1007/s10712-011-9119-1.
- Church, J. A., et al. (2013), Sea level change, in *Climate Change 2013: The Physical Science Basis. Contribution of Working Group I to the Fifth Assessment Report of the Intergovernmental Panel on Climate Change*, edited by T. F. Stocker et al., chap. 13, Cambridge Univ. Press, Cambridge, U. K., and New York.
- Compo, G. B., et al. (2011), The twentieth century reanalysis project, *Q. J. R. Meteorol. Soc.*, 137, 1–28, doi:10.1002/qj.776.
- Dangendorf, S., C. Mudersbach, T. Wahl, and J. Jensen (2013), Characteristics of intra-, inter-annual and decadal variability and the role of meteorological forcing: The long record of Cuxhaven, *Ocean Dyn.*, 63(2–3), 209–224, doi:10.1007/s10236-013-0598-0.
- Dangendorf, S., T. Wahl, E. Nilson, B. Klein, and J. Jensen (2014), A new atmospheric proxy for sea level variability in the south-eastern North Sea: Observations and future ensemble predictions, *Clim. Dyn.*, 43, 447–467, doi:10.1007/s00382-013-1932-4.
- Eichner, J. F., E. Koscielny-Bunde, A. Bunde, S. Havlin, and H. J. Schellnhuber (2003), Power-law persistence and trends in the atmosphere: A detailed study of long temperature records, *Phys. Rev. E*, 68(4), 046133.
- Franzke, C. L. E. (2012a), Nonlinear trends, long-range dependence and climate noise properties of surface air temperature, *J. Clim.*, 25, 4172–4183.
- Franzke, C. L. E. (2012b), On the statistical significance of surface air temperature in the Eurasian Arctic region, *Geophys. Res. Lett.*, 39, L23705, doi:10.1029/2012GL054244.
- Gehrels, W. R., and P. L. Woodworth (2013), When did modern rates of sea-level rise start?, *Global Planet. Change*, 100, 263–277.
- Greatbach, R. J. (1994), A note on the representation of steric sea level in models that conserve volume rather than mass, *J. Geophys. Res.*, 99(12), 767–12.
- Haigh, I. D., T. Wahl, R. M. Price, C. Pattiaratchi, C. M. Calafat, and S. Dangendorf (2014), Timescales for detecting a significant acceleration in sea level rise, *Nat. Commun.*, 5, 3635, doi:10.1038/ncomms4635.
- Hallegratte, S., C. Green, R. J. Nicholls, and J. Corfee-Morlot (2013), Future flood losses in major coastal cities, *Nat. Clim. Change*, 3, 802–806.
- Holgate, S. J., A. Matthews, P. L. Woodworth, L. J. Rickards, M. E. Tamisiea, E. Bradshaw, P. R. Foden, K. M. Gordon, S. Jevrejeva, and J. Pugh (2013), New data systems and products at the Permanent Service for Mean Sea Level, *J. Coast. Res.*, 29, 493–504, doi:10.2112/JCOASTRES-D-12-00175.1.
- Houston, J. R., and R. G. Dean (2011), Sea-level acceleration based on U.S. tide gauges and extension of previous global-gauge analyses, *J. Coast. Res.*, 27(3), 409–417.
- Hurst, H. E. (1951), Long term storage capacity of reservoirs, *Trans. Am. Soc. Civ. Eng.*, 116, 770–799.
- Jevrejeva, S., A. Grinsted, J. C. Moore, and S. Holgate (2006), Nonlinear trends and multiyear cycles in sea level records, *J. Geophys. Res.*, 111, C09012, doi:10.1029/2005JC003229.
- Kantelhardt, J. W., E. Koscielny-Bunde, H. A. Rego, S. Havlin, and A. Bunde (2001), Detecting long-range correlations with detrended fluctuation analysis, *Phys. A*, 295, 441–454.
- Kantelhardt, J. W., E. Koscielny-Bunde, D. Rybski, P. Braun, A. Bunde, and S. Havlin (2006), Long-term persistence and multifractality of precipitation records and river runoff records, *J. Geophys. Res.*, 111, D01106, doi:10.1029/2005JD005881.
- Koscielny-Bunde, E., H. E. Roman, A. Bunde, S. Havlin, and H. J. Schellnhuber (1998), Long-range power-law correlations in local daily temperature fluctuations, *Phil. Mag. B*, 77, 1331–1340.
- Lennartz, S., and A. Bunde (2009), Trend evaluation in records with long-term memory; application to global warming, *Geophys. Res. Lett.*, 36, L16706, doi:10.1029/2009GL039516.
- Levermann, A., P. U. Clark, B. Marzeion, G. A. Milne, D. Pollard, V. Radic, and A. Robinson (2013), The multimillennial sea-level commitment of global warming, *Proc. Natl. Acad. Sci. U.S.A.*, 110, 13,745–13,750.
- Ludescher, J., M. I. Bogachev, J. W. Kantelhardt, A. Y. Schumann, and A. Bunde (2011), On spurious and corrupted multifractality: The effects of additive noise, short-term memory and periodic trends, *Phys. A*, 390, 2480–2490.
- Marzeion, B., A. H. Jarosch, and M. Hofer (2012), Past and future sea-level change from the surface mass balance of glaciers, *Cryosphere*, 6, 1295–1322.
- Monetti, R. A., S. Havlin, and A. Bunde (2003), Long-term persistence in the sea surface temperature fluctuations, *Physica A: Statistical Mechanics and its Applications*, 320, 581–589, doi:10.1016/S0378-4371(02)01662-X.
- Peltier, W. R. (2004), Global glacial isostasy and the surface of the ice-age Earth: The ICE-5G(VM2) model and GRACE, *Ann. Rev. Earth. Planet. Sci.*, 32, 111–149.
- Peng, C. K., S. V. Buldyrev, S. Havlin, M. Simons, H. E. Stanley, and A. L. Goldberger (1994), Mosaic organization of DNA nucleotides, *Phys. Rev. E*, 49(2), 1685–1689.
- Piecuch, C. G., and R. M. Ponte (2012), Bouyancy-driven interannual sea level changes in the southeast tropical pacific, *Geophys. Res. Lett.*, 39, L05607, doi:10.1029/2012GL051130.
- Rohling, E. J., I. D. Haigh, G. L. Foster, A. P. Roberts, and K. M. Grant (2013), A geological perspective on potential future sea-level rise, *Nat. Sci. Rep.*, 3, 3461, doi:10.1038/srep03461.
- Rybski, D., and A. Bunde (2009), On the detection of trends in long-term correlated records, *Phys. A*, 388, 1687–1695.
- Rybski, D., A. Bunde, and H. von Storch (2008), Long-term memory in 1000 years simulated temperature records, *J. Geophys. Res.*, 113, D02106, doi:10.1029/2007JD008568.
- Sallenger, A. H., K. S. Doran, and P. A. Howd (2012), Hotspot of accelerated sea-level on the Atlantic coast of North America, *Nat. Clim. Change*, 2, 887–888.
- Slangen, A. B. A., M. Carson, C. A. Katsman, R. S. W. van de Wal, A. Köhl, L. L. A. Vermeersen, and D. Stammer (2014), Projecting twenty-first century regional sea-level changes, *Clim. Change*, doi:10.1007/s10584-014-1080-9.
- Stammer, D., A. Cazenave, R. M. Ponte, and M. E. Tamisiea (2013), Causes for contemporary sea level changes, *Annu. Rev. Mar. Sci.*, 5, 21–46.
- Trenberth, E. K. (2010), The ocean is warming, isn't it?, *Nature*, 465, 304–304, doi:10.1038/465304a.
- Woodworth, P. L., N. J. White, S. Jevrejeva, S. J. Holgate, J. A. Church, and W. R. Gehrels (2009), Evidence for the accelerations of sea level rise on multi-decade and century timescales, *Int. J. Climatol.*, 29, 777–789, doi:10.1002/joc.1771.